Multivariable Dynamic Ankle Mechanical Impedance With Active Muscles

Hyunglae Lee, *Member, IEEE*, Hermano Igo Krebs, *Fellow, IEEE*, and Neville Hogan

***Abstract*—Multivariable dynamic ankle mechanical impedance in two coupled degrees-of-freedom (DOFs) was quantified when muscles were active. Measurements were performed at five different target activation levels of tibialis anterior and soleus, from 10% to 30% of maximum voluntary contraction (MVC) with increments of 5% MVC. Interestingly, several ankle behaviors characterized in our previous study of the relaxed ankle were observed with muscles active: ankle mechanical impedance in joint coordinates showed responses largely consistent with a second-order system consisting of inertia, viscosity, and stiffness; stiffness was greater in the sagittal plane than in the frontal plane at all activation conditions for all subjects; and the coupling between dorsiflexion–plantarflexion and inversion–eversion was small—the two DOF measurements were well explained by a strictly diagonal impedance matrix. In general, ankle stiffness increased linearly with muscle activation in all directions in the 2-D space formed by the sagittal and frontal planes, but more in the sagittal than in the frontal plane, resulting in an accentuated "peanut shape." This characterization of young healthy subjects' ankle mechanical impedance with active muscles will serve as a baseline to investigate pathophysiological ankle behaviors of biomechanically and/or neurologically impaired patients.**

***Index Terms*—Ankle joint, ankle joint stiffness, ankle stiffness, human ankle, impedance structure, multivariable impedance, multivariable stiffness, stiffness anisotropy.**

I. Introduction

FOR the past few decades, human ankle impedance[1] has been studied extensively, given its significant roles in lower-extremity motor functions; devices providing external energy input to the ankle have enabled direct measurement of impedance, unavailable from traditional gait lab environments. Sinusoidal torque input was used in an early ankle impedance study [1]. The static or quasi-static component of ankle impedance, i.e., the torque-angle relationship at the ankle, was quantified for healthy and neurologically impaired patients using slow ramp perturbations [2]. Rapid ramp and hold perturbations have also been widely used to characterize both intrinsic and reflex ankle stiffness [3]–[5]. Stochastic system identification techniques have been used to examine viscoelastic and inertial components of ankle impedance; the effects of mean ankle position, mean ankle torque, and input displacement amplitude were thoroughly investigated [6]–[11]. Extension of stochastic system identification methods by integrating a nonlinear reflex pathway enabled separate identification of intrinsic and reflex components [12], [13]. While most previous ankle studies were confined to the sagittal plane, only a few studies reported quantification of impedance in the frontal plane [14]–[16], but still limited to a single degree-of-freedom (DOF).

The human ankle is a complicated joint involving multiple bones, ligaments, tendons, and muscles, and neural commands from the brain and spinal reflex feedback may further complicate actions of the ankle joint in multiple DOFs. In fact, single DOF ankle movements are unusual in normal lower-extremity functions, including walking [17]. We believe that characterizing multivariable ankle impedance promises deeper understanding of its roles in motor control and function, not achievable from single DOF studies. Separate measurements of passive ankle stiffness in inversion–eversion (IE) and dorsiflexion–plantarflexion (DP) were reported previously but coupling between DOFs was not addressed [18], [19]. We previously reported ankle impedance in two coupled DOFs simultaneously, in both the sagittal and frontal planes. We performed static studies with muscles relaxed [20] and active [21] to characterize the nonlinear torque-angle relation at the ankle, from which we showed the directional variation of static ankle impedance; and that contributions of inter-muscular reflex feedback resulted in a largely spring-like, conservative behavior for our unimpaired subjects. In addition, we conducted a static study with neurologically impaired patients, demonstrating that their ankle impedance can be substantially different from that of unimpaired control subjects, even with relaxed muscles [22]. However, these studies were confined to characterization of the static component of impedance. To overcome that limitation, we performed dynamic studies to characterize multivariable ankle impedance in the frequency domain [23]–[25]. Ankle impedance with relaxed muscles was characterized as a function of frequency in joint coordinates, defined by IE and DP

Manuscript received September 17, 2013; revised February 07, 2014; accepted May 27, 2014. Date of publication June 04, 2014; date of current version September 04, 2014. This work was supported in part by Toyota Motor Corporation's Partner Robot Division and in part by the National Institutes of Health (NIH) under R01 HD069776. The work of H. Lee was supported by a Samsung Scholarship.

H. Lee was with the Department of Mechanical Engineering, Massachusetts Institute of Technology, Cambridge, MA 02139 USA. He is now with the Sensory Motor Performance Program, Rehabilitation Institute of Chicago, Chicago, IL 60611 USA (e-mail: hyunglae@alum.mit.edu).

H. I. Krebs is with the Mechanical Engineering Department, Massachusetts Institute of Technology, Cambridge, MA 02139 USA, and also with the Department of Neurology and the Division of Rehabilitative Medicine, University of Maryland School of Medicine, Baltimore, MD 21201 USA (e-mail: hikrebs@mit.edu).

N. Hogan is with the Mechanical Engineering Department, and Brain and Cognitive Science Department, Massachusetts Institute of Technology, Cambridge, MA 02139 USA (e-mail: neville@mit.edu).

Color versions of one or more of the figures in this paper are available online at http://ieeexplore.ieee.org.

Digital Object Identifier 10.1109/TNSRE.2014.2328235

[1]For brevity, we often omit the "mechanical" prefix.

Fig. 1. Experimental setup. Left: Anklebot setup. Right: Measurements in the seated posture.

directions. Despite its internal complexity, externally simple ankle behavior was consistently observed, including minimal coupling between DOFs even though there was substantial directional variation of ankle impedance [24]. While that study serves as a valuable baseline, normal lower-extremity actions generally involve multiple levels of muscle activation.

II. Methods

A. Experimental Setup and Protocol

The same experimental setup used in our previous study [24], a wearable ankle robot, Anklebot (Interactive Motion Technologies, Inc.) [18], and a surface electromyographic (EMG) system (Myomonitor IV, Delsys Inc.), were used in this study. The body of the robot was mounted to a knee brace and two actuators of the robot were connected to a rigid U-shaped bracket attached to the bottom of a custom designed shoe [Fig. 1(left)]. Anklebot provided actively controllable torques in two DOFs, in both IE and DP, and the third DOF (axial rotation) was passive to prevent imposing inadvertent kinematic constraints at the ankle. Each motor (Kollmorgen RBE(H) 00714) was operated under current control and torques were reliably estimated from motor currents, measured using a digital-to-analog converter (United Electronic Industries PD2-AO-8/16) with 16 bit resolution. Torque sensitivity, the relationship of output torque to motor input current, was characterized for each motor under dynamic conditions, and was verified by measurements from a load cell transducer [18]. Torque and angular displacement of each motor were transformed to force and linear displacement through a linear drive (Rohlix; backlash less than 2.6×10^{-5} m). Displacements of these linear actuators were measured with two optical linear encoders (Renishaw; resolution 5×10^{-6} m), then fed into a PCI interface card (US Digital PCI-4E-D) and low-pass filtered (100 Hz cutoff; 20 dB/decade roll-off). Actuator force and displacement were recorded at 1 kHz and transformed to angular displacements and torques at the ankle in IE and DP through a nonlinear kinematic transformation [20]. Torque rather than position perturbations were used to avoid excessive displacement of the ankle during high muscle activation tasks; using torque perturbations the subject had control over ankle position, determined by the admittance of the ankle and environment [26]. Surface EMG electrodes (Myomonitor IV, DELSYS) were placed over the bellies of four major ankle muscles: tibialis anterior (TA), peroneus longus (PL), soleus (SOL), and lateral gastrocnemius (GAS). Surface EMG signals were band-pass filtered between 20 and 450 Hz and sampled at 1 kHz. Amplitudes of EMG signals were estimated using a root-mean-square average with a moving window of 200 ms after removing the dc bias offsets [27]. The MVC level of each muscle was measured following procedures described in [28], which was used as a reference to normalize EMG amplitudes.

After MVC measurements, subjects were seated in a chair wearing a knee brace and a custom designed shoe. Multiple Velcro straps of the knee brace, which covered from the lower part of calf muscles up to approximately the middle part of thigh muscles, were tightly fastened to prevent relative movements of the knee brace with respect to the leg. A proper shoe size was selected for each subject, the foot was securely tied with shoe laces, and a wide Velcro strap was wrapped around over the laces to minimize foot slippage inside the shoe. Then the robot was attached to the knee brace and the shoe, and the initial neutral position of the ankle was set when the foot and shank formed a right angle. The leg and the robot were suspended by elastic bands to support the weight of the robot. The use of a compliant elastic support also helped to minimize possible artifacts due to the coupling of the leg and the robot to surrounding structures, including the chair, by moving possible artifactual resonant modes to well below the frequency we measured [Fig. 1(right)].

For dorsiflexor and plantarflexor active studies, TA and SOL were selected as target muscles, respectively. Ankle impedance was measured at five different activation levels for each study, from 10% to 30% of MVC level with increments of 5% MVC. To prevent muscle fatigue, at least a 3 min rest period was given between measurements. As a baseline for active studies, passive ankle impedance was also measured with fully relaxed muscles. During measurements, a visual feedback display showing current and target activation levels was provided to subjects. Subjects were first instructed to activate a specific muscle and maintain it at the target level. When the activation level reached the target level, the robot applied mild random torque perturbations (band-limited white noise with a spectrum flat up to 100 Hz) to the ankle for 40 s for each measurement.

Ten unimpaired young human subjects (five males, five females; all right footed) with no reported history of neuromuscular or biomechanical disorders participated in this study (the same subject group as in [24]). Subjects were between the ages of 21–37, heights of 1.58–1.90 m, and weights 48.0–80.0 kg. Following procedures pre-approved by MIT's institutional review board, the Committee on the Use of Humans as Experimental Subjects, informed consent was obtained from all subjects.

B. Multivariable Ankle Mechanical Impedance Identification and Its Relationship to Muscle Activation

Multivariable ankle impedance in joint coordinates ($\boldsymbol{Z} = [Z_{11}, Z_{12}; Z_{21}, Z_{22}]$, where subscripts 1 and 2 denote IE and DP, respectively) was identified by linear time-invariant (LTI) multi-input multi-output (MIMO) system identification

methods based on spectral analysis [29], [30]. The same controller as in our previous relaxed study [24] was implemented for each actuator, combining a proportional controller and random perturbations, except with different gain settings for measurements with active muscles; the gain of the controller, which determined the Anklebot stiffness, was set to 2000 N/m to hold the ankle near its initial neutral position against ankle torques due to muscle activation. In joint coordinates, this corresponds to 37.2 Nm/rad and 76.0 Nm/rad for IE and DP, respectively. In estimating ankle impedance, the contribution of actuator dynamics was compensated by subtracting Anklebot impedance, measured by running the same identification protocol but without a human subject, from the measured impedance.

A partial coherence matrix ($\mathbf{\Omega}^2 = [\Omega_{11}^2, \Omega_{12}^2; \Omega_{21}^2, \Omega_{22}^2]$) was calculated based on spectral analysis [29], [30] to investigate the validity of the LTI system identification approach as well as to quantify the amount of coupling between the two DOFs. The reliability of identification was also evaluated in the time domain by calculating the percentage variance accounted for (%VAF) between output measurements and predicted outputs from identified impedances. To be precise, output predictions were estimated by the convolution of torque inputs and admittance impulse response functions, the latter calculated by inverse discrete Fourier transform of the admittances from the closed-loop identification [24]. To quantify how well a simple second-order model consisting of rotational inertia, viscosity, and stiffness fit the identification results, the best-fit model was selected by minimizing mean-squared-error between the identified open-loop impedance and the impedance of the best-fit model over a frequency range between 1 and 20 Hz. Then, the %VAF between output predictions from the identified impedance and the fitted model was calculated [24].

Next, to characterize the directional variation (anisotropy) of ankle impedance in the 2-D space formed by IE and DP, the same impedance identification procedure was repeated in rotated joint coordinates with 10° increments of rotation angle. Results were presented as a function of frequency in 3-D plots, where one axis denoted the frequency and the angle and radius in the plane perpendicular to that axis respectively indicated the movement direction in the IE-DP space and the impedance magnitude in that direction. In addition, a single representative directional variation was obtained by averaging the shapes below a specific frequency (in this paper below 10 Hz). Directions of major and minor principal axes, exhibiting the greatest and least impedance magnitude, were calculated. Finally, to investigate the relationship between muscle activation and the corresponding ankle impedance, the correlation coefficient (R^2) was calculated for each movement direction in the 2-D space.

III. Results

A. EMG Analysis

All subjects successfully maintained relaxed muscles during the measurement of baseline passive impedance. When EMG amplitudes were scaled to their corresponding MVC, the normalized activation levels were under 0.3% MVC when averaged across all subjects. In the active muscle studies, the normalized EMG amplitude of each measurement was compared with the corresponding target level (10%–30% MVC) to ensure that each subject was able to follow instructions and maintain target muscle activation levels. Target levels for the TA were well maintained, while activation levels of the SOL were slightly higher than the target levels [Fig. 2(a)]. Besides target muscle activation, we also evaluated total ankle muscle activation because all ankle muscles including the target muscle contribute to ankle joint impedance. In fact, subjects did not solely activate a single muscle, but evoked a degree of co-activation of other muscles due to synergies [31]. For example, when SOL was the target muscle, all measured plantarflexors (SOL, PL, and GAS) were activated in the same pattern, while TA activation was very low [Fig. 2(a)]. The total muscle activation was approximated by summing normalized EMG amplitudes of all measured muscles.

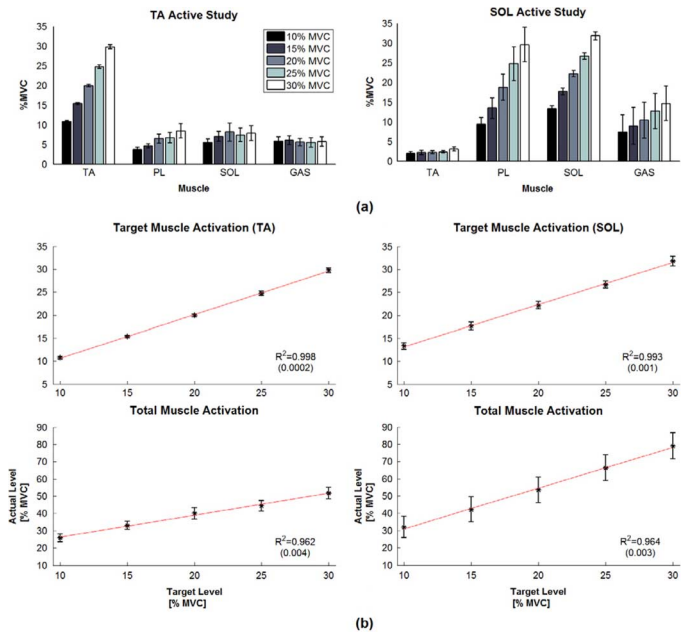

Fig. 2. Muscle activation levels and the linearity between target and actual muscle activation. (a) Normalized muscle activation levels (%MVC) of all measured muscles. (b) Linearity of normalized muscle activation levels. Left column: TA active study, right column: SOL active study. Top row: target muscle activation, bottom row: total muscle activation. Mean and mean ± standard error (SE) of all subjects are illustrated as asterisks and bars. Red lines are linear regression fits to measurements. Correlation coefficient (R^2) was calculated for each subject and averaged across all subjects.

The linearity of actual muscle activation levels was evaluated by calculating the correlation coefficient (R^2) between target and actual muscle activation levels. In both the TA and SOL active studies, all subjects showed very high R^2 values, close to 1 for both target muscle and total muscle activation [Fig. 2(b)]. In fact, even the lowest R^2 value for any individual subject was 0.98 and 0.90 for target and total muscle activation, respectively.

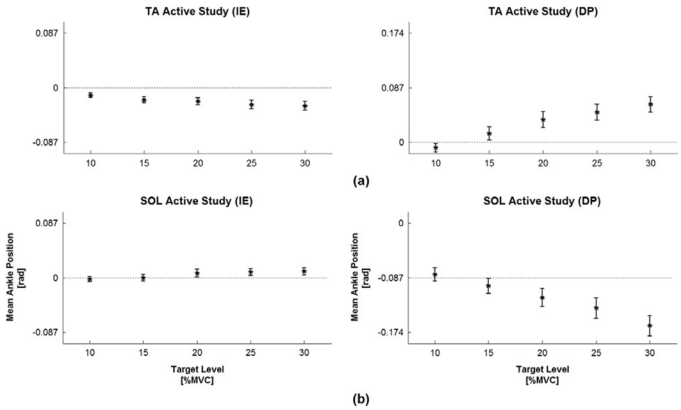

Fig. 3. Mean ankle position in active muscle studies. (a) TA active study, (b) SOL active study. Positive (negative) values denote dorsiflexion (plantarflexion) and eversion (inversion) in the sagittal and the frontal planes, respectively. Mean and mean ± SE of all subjects are illustrated as asterisks and bars.

B. Ankle Mechanical Impedance in Joint Coordinates

As expected, different levels of muscle activation caused different mean ankle positions. Since it has been shown that ankle impedance varies with mean ankle position [9], [10], it is important to note the ranges of ankle positions measured in the experiment. Across all muscle activation conditions, the ankle was constrained to a small range of motion (ROM) due to high restoring torques by the robot in both DOFs: -0.028–-0.012 rad (IE) and -0.009–0.061 rad (DP) for the TA active study [Fig. 3(a)], and -0.002–0.011 rad (IE) and -0.164–-0.082 rad (DP) for the SOL active study [Fig. 3(b)].

In all muscle activation conditions the diagonal elements of the partial coherence matrix (Ω^2_{11} and Ω^2_{22}) were high up to 50 Hz, except at low frequencies below 1–2 Hz, where the partial coherences decreased as muscle activation increased. On the other hand, the off-diagonal elements (Ω^2_{12} and Ω^2_{21}) were low (Fig. 4). This could be due to departure from linearity or a lack of coupling between DOFs. The former was ruled out by evaluating the %VAF between measured outputs and outputs predicted from only the diagonal components of the identified impedances (Z_{11} and Z_{22}). When averaged across all subjects, the %VAF was greater than 89% and 84% in the IE and DP directions, respectively, under all muscle activation conditions (Table I). Since off-diagonal impedances were not reliable due to low off-diagonal coherences, they were excluded from further analyses.

The diagonal elements of the ankle impedance matrix, i.e., IE and DP impedances (Z_{11} and Z_{22}), are shown as Bode plots (Fig. 5). For both directions and for all muscle activation conditions, inertia was dominant (magnitude increased at ~ 40 dB/dec) at frequencies over about 10–20 Hz depending on muscle activation. Below this region, stiffness was dominant (magnitude slope $\sim$ 0 dB/dec) though it increased with the level of muscle activation. Identified results were well approximated by a simple second-order model consisting of rotational inertia, viscosity, and stiffness; the %VAF between

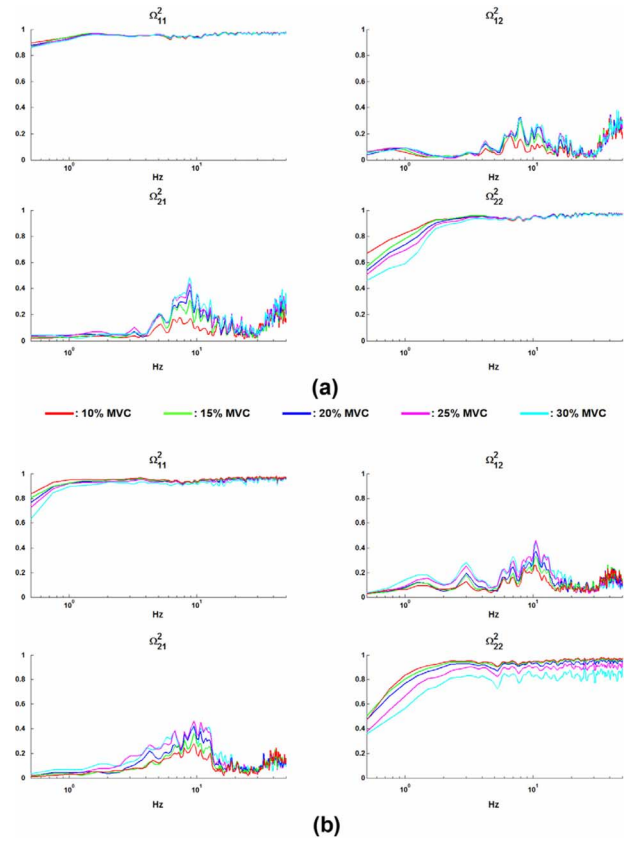

Fig. 4. Partial coherences in joint coordinates. (a) TA active study. (b) SOL active study. Red, green, blue, magenta, and cyan colors denote results at target level 10%, 15%, 20%, 25%, and 30% MVC, respectively. Means of all subjects are presented.

TABLE I
RELIABILITY OF IDENTIFICATION (%VAF) AND GOODNESS OF FIT OF SECOND-ORDER MODEL APPROXIMATION ($\%\mathrm{VAF}_{\mathrm{model}}$)

%*VAF*				
Study	TA Active Study		SOL Active Study	
Direction / Target level	IE	DP	IE	DP
10% MVC	94.7 (0.05)	91.8 (0.24)	94.3 (0.15)	91.6 (0.41)
15% MVC	94.6 (0.06)	90.9 (0.32)	93.4 (0.28)	90.2 (0.54)
20% MVC	94.3 (0.11)	89.4 (0.45)	92.6 (0.34)	86.7 (0.93)
25% MVC	94.1 (0.15)	88.6 (0.48)	91.2 (0.33)	87.5 (0.82)
30% MVC	93.8 (0.17)	88.3 (0.42)	89.4 (0.36)	84.2 (0.91)
$\%VAF_{model}$				
10% MVC	99.0 (0.07)	99.1 (0.09)	99.1 (0.01)	99.0 (0.05)
15% MVC	98.7 (0.16)	98.9 (0.18)	99.2 (0.03)	98.7 (0.07)
20% MVC	98.7 (0.16)	98.7 (0.40)	99.0 (0.07)	98.7 (0.11)
25% MVC	98.6 (0.12)	98.5 (0.27)	99.1 (0.04)	98.4 (0.22)
30% MVC	98.6 (0.15)	98.4 (0.24)	99.2 (0.03)	97.5 (0.27)

The mean and the SE (value in parentheses) across all subjects are presented (Unit: %).

displacement outputs predicted from the identified impedance and outputs predicted from the best-fit model ($\%\mathrm{VAF}_{\mathrm{model}}$) was higher than 97.5% (Table I). Identified ankle parameters are summarized in Table II. As expected, ankle inertias (I_{11} and I_{22}) were essentially invariant across all muscle activation conditions–magnitude responses in the high frequency region

TABLE II
ANKLE PARAMETERS FROM SECOND-ORDER MODEL APPROXIMATION

Study	TA Active Study					
Direction	IE			DP		
Parameters / Target Level	I_{11}	B_{11}	K_{11}	I_{22}	B_{22}	K_{22}
10% MVC	0.002 (0.0001)	0.19 (0.01)	12.1 (0.3)	0.006 (0.0002)	0.74 (0.02)	41.5 (1.0)
15% MVC	0.002 (0.0001)	0.23 (0.01)	15.0 (0.4)	0.006 (0.0002)	0.86 (0.02)	53.7 (1.6)
20% MVC	0.002 (0.0001)	0.25 (0.01)	17.1 (0.5)	0.006 (0.0002)	0.94 (0.02)	63.1 (2.1)
25% MVC	0.003 (0.0001)	0.27 (0.01)	19.5 (0.5)	0.007 (0.0003)	1.04 (0.03)	71.9 (2.2)
30% MVC	0.003 (0.0001)	0.30 (0.01)	21.3 (0.5)	0.007 (0.0004)	1.08 (0.03)	79.4 (2.5)
Study	SOL Active Study					
Direction	IE			DP		
Parameters / Target Level	I_{11}	B_{11}	K_{11}	I_{22}	B_{22}	K_{22}
10% MVC	0.002 (< 0.0001)	0.23 (0.01)	13.7 (0.8)	0.006 (0.0001)	0.66 (0.02)	45.3 (2.1)
15% MVC	0.003 (0.0001)	0.30 (0.01)	18.0 (1.3)	0.007 (0.0002)	0.82 (0.02)	56.1 (2.4)
20% MVC	0.003 (0.0001)	0.37 (0.02)	22.7 (1.6)	0.007 (0.0004)	0.97 (0.03)	69.2 (3.1)
25% MVC	0.003 (0.0001)	0.43 (0.02)	27.3 (1.6)	0.006 (0.0002)	1.06 (0.04)	88.3 (5.6)
30% MVC	0.003 (0.0001)	0.52 (0.02)	36.4 (1.8)	0.007 (0.0003)	1.29 (0.04)	118.5 (7.7)

The mean and SE (value in parentheses) across all subjects are presented. Units for I, B, K are kgm^2, Nms/rad, Nm/rad, respectively.

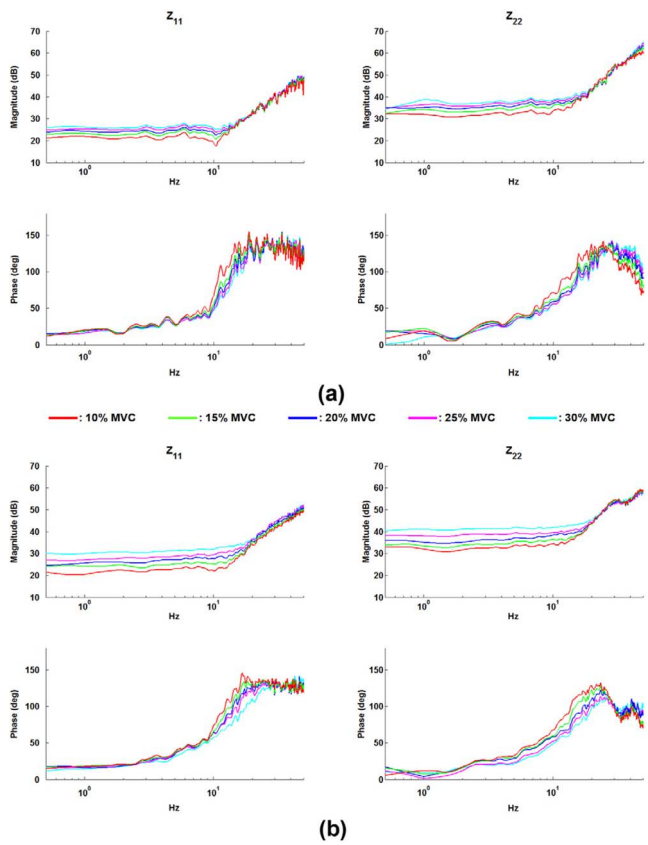

Fig. 5. Ankle mechanical impedance in joint coordinates. (a) TA active study, (b) SOL active study. Left: IE impedance (Z_{11}), Right: DP impedance (Z_{22}). Top: magnitude response, Bottom: phase response, respectively. Same color codes as in Fig. 4. Resonance and anti-resonance behavior over about 20–30 Hz was due to vibration of the bracket of the shoe, as explained in [24].

were on top of each other (Fig. 5). On the other hand, viscosity (B_{11} and B_{22}), and stiffness (K_{11} and K_{22}) parameters increased with muscle activation.

C. Directional Variation (Anisotropy) of Ankle Mechanical Impedance With Active Muscles

The directional variation of ankle impedance was identified from calculations in rotated joint coordinates($\theta'_{\mathrm{IE}}, \theta'_{\mathrm{DP}}$). The increment of the rotation angle (α) was 10° ($\alpha = 0°, 10°, \ldots, 80°$). The input power spectral density (PSD) was first estimated in the rotated joint coordinates. The PSDs of τ'_{IE} and τ'_{DP} were flat up to 100 Hz for any α, validating that ankle impedance can be reliably estimated in all directions in the IE-DP space using spectral analysis. The directional variation of ankle impedance was evaluated as a function of frequency, and results were averaged over a window between 1 and 10 Hz, where stiffness was dominant. Measurements below 1 Hz were not considered since partial coherences below 1 Hz were low (Fig. 4). Remarkably, the shape of anisotropy was consistent over these frequencies and under different levels of muscle activation; weaker impedance in IE than DP resulted in a characteristic "peanut" shape (Fig. 6). In addition, the principal axes were slightly tilted in the counter-clockwise (CCW) direction (Fig. 6).

Considering the small variation at frequencies below 10 Hz, a single representative stiffness structure was obtained by averaging results in this region (Fig. 7). Activating muscles significantly increased ankle stiffness in all directions in the IE-DP space, but it increased more in DP than in IE, accentuating the "peanut" shape, pinched in the IE direction. Although the amount of stiffness increase was greater in DP than IE, the ratio of DP stiffness to IE stiffness did not change significantly with muscle activation level (Table III); pooling all subjects' data for each muscle activation level, the ratio satisfied normality conditions ($p > 0.05$ according to a Jarque-Bera test, MATLAB's jbtest function), and a one-way analysis of variance (MATLAB's anova1 function) showed no statistical difference ($p \gg 0.05$). In addition, the ratio of stiffness in active studies to passive (maximally-relaxed) stiffness was calculated for each movement direction (Table III); the ratio in IE was substantially lower than in DP for each activation level, implying

TABLE III
DIRECTIONAL VARIATION OF ANKLE STIFFNESS WITH ACTIVE MUSCLES

The ratio of DP stiffness to IE stiffness		
Study / Target Level	TA Active Study	SOL Active Study
10% MVC	3.62 (0.16)	3.56 (0.40)
15% MVC	3.75 (0.17)	3.61 (0.44)
20% MVC	3.78 (0.18)	3.58 (0.51)
25% MVC	3.79 (0.17)	3.54 (0.51)
30% MVC	3.78 (0.19)	3.35 (0.45)

The ratio of total (passive+active) stiffness to passive stiffness						
Study	TA Active Study			SOL Active Study		
Direction / Target Level	IE	DP	All	IE	DP	All
10% MVC	1.60 (0.13)	3.15 (0.25)	2.49 (0.19)	1.87 (0.10)	3.41 (0.50)	2.75 (0.38)
15% MVC	2.03 (0.19)	4.11 (0.37)	3.22 (0.28)	2.46 (0.17)	4.23 (0.58)	3.46 (0.49)
20% MVC	2.32 (0.21)	4.84 (0.49)	3.76 (0.36)	3.11 (0.22)	5.22 (0.75)	4.30 (0.65)
25% MVC	2.65 (0.22)	5.49 (0.50)	4.27 (0.37)	3.73 (0.22)	6.66 (1.33)	5.38 (0.98)
30% MVC	2.91 (0.24)	6.05 (0.57)	4.70 (0.42)	4.98 (0.25)	8.94 (1.83)	7.21 (1.32)

The mean and SE (in parentheses) across all subjects are presented in the table. All implies the mean of all 36 directions.

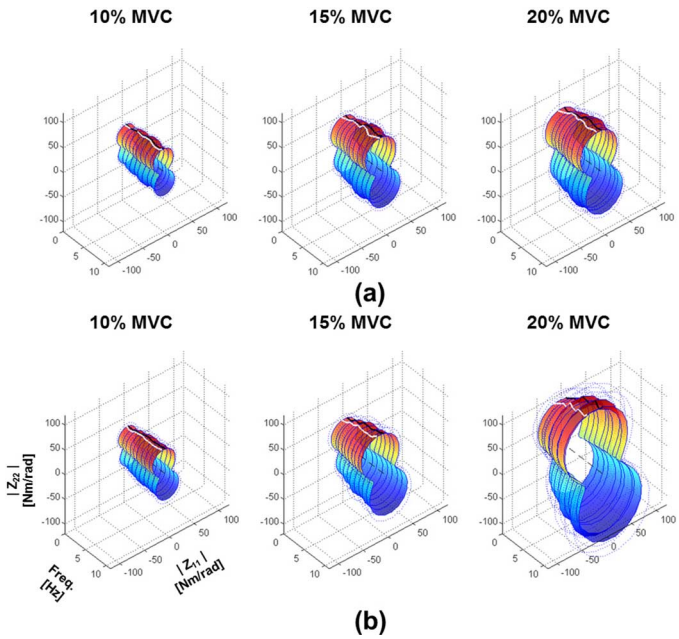

Fig. 6. Directional variation (anisotropy) of ankle mechanical impedance as a function of frequency. (a) TA active study. (b) SOL active study. First, second, and third columns correspond to 10% MVC, 20% MVC, and 30% MVC, respectively. Blue solid and dotted lines represent the mean and mean ±1 SE of all subjects, respectively. Black and white lines correspond to the directions of dorsiflexion and the major principal axis.

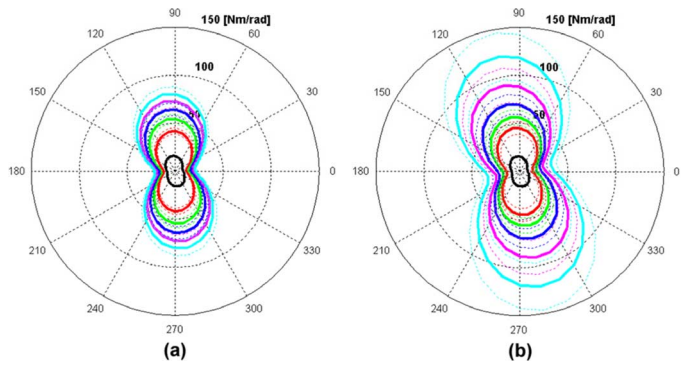

Fig. 7. Directional variation (anisotropy) of ankle stiffness. Angle denotes movement direction in the 2-D space and the radius represents the magnitude of impedance in the movement direction. Right foot eversion, dorsiflexion, inversion, and plantarflexion, correspond to 0°, 90°, 180°, and 270°, respectively. Same color codes, as in Fig. 4.

TABLE IV
ANKLE STIFFNESS IN PRINCIPAL AXIS DIRECTIONS

	Direction of principal axes [rad]	Stiffness in the major axis direction [Nm/rad]	Stiffness in the minor axis direction [Nm/rad]	Ratio of stiffness between major and minor axis directions
Study / Target	TA Active Study			
10% MVC	0.05 (0.03)	41.8 (3.3)	11.6 (1.0)	3.7 (0.2)
15% MVC	0.10 (0.03)	54.8 (4.9)	14.6 (1.4)	3.8 (0.2)
20% MVC	0.09 (0.03)	64.4 (6.5)	16.7 (1.6)	3.9 (0.2)
25% MVC	0.10 (0.03)	73.3 (6.8)	18.9 (1.6)	3.9 (0.2)
30% MVC	0.09 (0.03)	80.7 (7.7)	20.8 (1.7)	3.9 (0.2)
Study / Target	SOL Active Study			
10% MVC	0.09 (0.04)	46.0 (6.8)	12.9 (2.1)	3.8 (0.4)
15% MVC	0.16 (0.05)	57.8 (8.0)	16.2 (2.8)	3.9 (0.4)
20% MVC	0.17 (0.05)	72.0 (10.7)	19.8 (3.5)	3.9 (0.5)
25% MVC	0.23 (0.04)	91.8 (18.1)	23.8 (4.0)	4.0 (0.5)
30% MVC	0.23 (0.05)	122.6 (24.7)	32.3 (5.0)	3.9 (0.5)

Directions of principal axes are defined from DP in CCW direction (Unit of direction: rad, unit of stiffness: Nm/rad). The mean and SE (value in parentheses) over all subjects are presented.

that the relative contribution of passive stiffness to total stiffness (passive stiffness + active stiffness) was significantly higher in IE than DP. For both TA and SOL active studies, the directions of principal axes were slightly tilted CCW from the original joint coordinates across different muscle activation levels: 0.05–0.09 rad and 0.09–0.23 rad for TA and SOL studies, respectively, when averaged across all subjects (Table IV). As expected from comparing stiffness in the IE and DP directions, stiffness in the major principal axis direction was substantially larger than in the minor principal axis direction, and the ratio between them was remarkably invariant across subjects and across muscle activations.

The correlation coefficient (R^2) between the level of muscle activation and the corresponding ankle stiffness was calculated and presented in polar coordinates (Fig. 8). In the TA active study, R^2 values were very high: 0.94, 0.95, and 0.94 for IE,

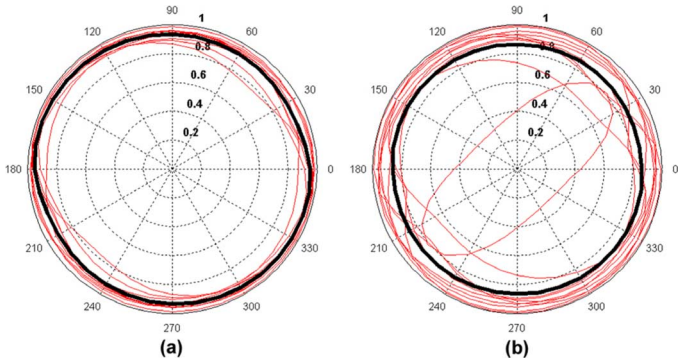

Fig. 8. Linearity between muscle activation level and ankle stiffness in IE-DP space. Correlation coefficient (R^2) for each movement direction is presented in polar coordinates. Each thin red line represents the result of an individual subject, and the thick black line represents the mean of all subjects. (a) TA active study. (b) SOL active study.

TABLE V
LINEARITY (R^2) BETWEEN MUSCLE ACTIVATION LEVEL AND ANKLE STIFFNESS

Study	TA Active Study			SOL Active Study		
Direction / Subject	IE	DP	All	IE	DP	All
1	0.97	0.96	0.95	0.99	0.93	0.93
2	0.98	0.95	0.96	0.95	0.99	0.97
3	0.95	0.96	0.95	0.84	1.00	0.94
4	0.94	0.88	0.88	0.96	0.91	0.91
5	0.91	0.88	0.89	0.96	0.93	0.94
6	0.96	0.96	0.95	0.44	0.41	0.49
7	0.89	0.97	0.91	0.88	0.96	0.93
8	0.98	0.94	0.96	0.94	0.90	0.93
9	0.98	0.91	0.93	0.86	0.74	0.78
10	0.98	0.99	0.98	0.81	0.90	0.86
Mean (SE)	0.94 (0.01)	0.95 (0.01)	0.94 (0.01)	0.87 (0.05)	0.87 (0.06)	0.87 (0.04)

All implies the mean of all 36 directions.

DP, and all movement directions, respectively (Table V), when averaged across all subjects. In the SOL active study, R^2 values were somewhat lower though still high: 0.87, 0.87, and 0.87 for IE, DP, and all movement directions, respectively. This was mainly due to one outlier subject (#6) who showed substantially lower R^2 values (Table V). When averaged excluding this subject, R^2 values were higher than 0.90 for IE, DP, and all movement directions.

IV. DISCUSSION

A. Importance and Validity of Experimental Procedure

Characterization of the ankle's multivariable dynamic mechanical impedance with active muscles is important to understand roles of the ankle in interaction with the physical world. Normal motor functions mainly involve multi-dimensional ankle motions, which are not confined to static conditions, and require muscle activation, either voluntarily or reflexively. While previous studies over the past few decades have been limited to characterization of the ankle in a single DOF, mostly in the sagittal plane with few in the frontal plane, the study reported here targeted impedance identification in two coupled DOFs. This provides a unique opportunity to investigate coupled 2-D ankle impedance. The current study extended our previous dynamic study [24] to overcome limitations of multivariable static studies [20], [21], and provided (to our knowledge) the first observations of how multivariable dynamic ankle impedance of intact subjects changes with muscle activation. This study also provides a baseline for clinical studies in patients, especially those with neurological impairments; further clinical implications are discussed in a concluding section.

Experimental procedures and analysis methods similar to our previous study [24] were successfully used to identify ankle impedance over a wide range of muscle activations from 10% to 30% of MVC with increments of 5% MVC for TA and SOL. The short measurement time and random nature of the perturbations enabled all subjects successfully to maintain TA or SOL activation near the five different target levels. A linear regression between observed and target muscle activation yielded high R^2 values for both target and total muscle activation. A closed-loop position controller with an appropriate gain constrained the ankle to a small ROM: the difference of mean ankle positions between 30% MVC and 10% MVC was less than 0.016 rad and 0.082 rad for IE and DP, respectively. Based on previous studies investigating the effect of mean ankle position on ankle impedance with relaxed [9], [32] and active muscles (TA or triceps surae) [10], we believe these different ankle positions had minimal effect on ankle impedance. Thus, the high linearity of muscle activation and tightly constrained ankle positions for all muscle activation levels validated the ability of our experimental setup and protocol to reliably investigate the effect of muscle activation on ankle impedance.

Analysis of partial coherences verified that the mild random torque perturbations used in this study were powerful enough to estimate ankle impedance in two DOFs even with muscle activations at 30% MVC. While the diagonal coherence values varied with contraction level (especially with SOL active), consistent with reduced displacements in response to perturbation, it remained high at frequencies above about 1 or 2 Hz. In both TA active and SOL active studies, increased muscle activation reduced the diagonal partial coherences in the region below about 1–2 Hz. Low coherence may be due to insufficient input power, measurement noise, contribution of unmeasured inputs, and/or a nonlinear input–output relationship. In this study, the most likely cause was increased nonlinearity due to greater contribution of active ankle muscles, whose intrinsic dynamics are nonlinear [33]. Reflex contributions, which may also introduce nonlinearity, may also increase with higher muscle activation as reported previously [34]–[36]. Further study seems warranted to investigate the relative contributions of reflex and intrinsic components of impedance in two DOFs. The linear identification method used here may be extended to include certain types of nonlinearity, as in the model-based parallel-cascade identification method [12], while retaining current experimental procedures with a wearable ankle robot applying random perturbations in multiple-DOFs. This extension may be especially important when studying the impaired ankle.

TABLE VI
STIFFNESS MAY NOT INCREASE WITH MUSCLE ACTIVATION

Target \ Direction	Stiffness ratio		Muscle activation ratio	
	IE	DP	Target Muscle Activation (SOL)	Total Muscle Activation
25% MVC	1.02	0.96	1.18	1.06
30% MVC	0.95	0.93	1.41	1.14

The ratio of stiffness and muscle activation level to the corresponding value at 20 %MVC of subject #6 are presented. Note that stiffness in both IE and DP is essentially unchanged (or declines) despite substantial increase in muscle activation.

B. Simple Characteristics of Multivariable Dynamic Ankle Impedance with Active Muscles

Ankle impedance in the IE and DP directions can be treated independently for our healthy young subjects. The %VAF between measured outputs and predictions from the diagonal components of identified impedances was very high (more than 89% and 84% for the IE and DP directions, respectively), indicating that the low off-diagonal coherences were due to small coupling between DOFs. In fact, off-diagonal partial coherences were low (< 0.2) at most frequencies, except in a region around 10 Hz. In this region, coherences were higher than those in the relaxed study [24], and increased with muscle activation. However, even the highest coherence value was still low (~ 0.4).

Based on high diagonal partial coherences, IE and DP impedances were reliably estimated. In all muscle activation conditions, estimates of both IE and DP impedances were largely consistent with a second-order model consisting of rotational inertia, viscosity, and stiffness ($> 97.5\%$) (Table I). This result should be interpreted with care because it indicates how much variance of the linear impedance estimates, not the real measurements, was explained by the best-fit second-order model.

Averaged across all subjects, stiffness (estimated by averaging the magnitude of impedance below 10 Hz) increased with the level of muscle activation (Fig. 5). Interestingly, one subject (#6) in the SOL active study was an outlier; this subject exhibited no stiffness increase at activation levels higher than 25% and 20% of MVC for IE and DP, respectively (Table VI). This was not due to a failure to activate muscles, which showed a linearly increasing trend for SOL ($R^2 = 0.995$) as well as for the sum of normalized EMG amplitudes of all four measured muscles ($R^2 = 0.955$). Instead, as detailed in an Appendix, this experimental observation may be explained by the apparent stiffness that arises from a nonlinear relation between muscle length and joint angle. For this subject (#6), constant stiffness at higher muscle activation may be attributed to a substantial contribution of negative kinematic stiffness; i.e., the ratio of muscle stiffness to muscle force was less than the ratio of kinematic stiffness to muscle force. Though observed in only one subject, this is important experimental confirmation of previous analysis showing that an increase of ankle impedance with muscle activation is not *a priori* obvious [37], [38].

Ankle impedance substantially increased with muscle activation in all directions in the 2-D space defined by rotations in the sagittal and frontal planes, but increased more in DP than IE, resulting in an accentuated "peanut shape" in both the TA active and SOL active studies. This characteristic shape was also consistently observed over a wide range of frequencies. Although IE impedance with active muscles was relatively weak compared to DP impedance, activation of ankle muscles increased IE impedance to a few times higher than its passive value. Thus, for healthy subjects, activation of ankle muscles may be a good strategy to improve lower-extremity lateral stability and avoid prevalent ankle injuries in IE [39], [40]. While active ankle stiffness increased more in DP than IE when compared to the corresponding passive stiffness, the ratio of stiffness in DP to IE was remarkably invariant across different muscle activation levels. This may be anticipated from musculo-skeletal kinematics. Any contribution of a muscle to both IE and DP should increase in proportion as the muscle is activated.

We observed a highly linear relation between muscle activation and ankle stiffness in all movement directions in the 2-D space; all subjects in the TA active study and all except one (#6) in the SOL active study exhibited high linearity; the low linearity for subject #6 was due to non-monotonically increasing ankle stiffness as explained above. This result indicates that, in general, the ankle stiffness of healthy young subjects could be accurately predicted solely from activation of ankle muscles, even with the existence of potentially confounding kinematic stiffness. The simple relation between muscle activation and corresponding ankle impedance is important, because it will enable us to estimate ankle impedance based on muscle activation when direct measurement is not feasible or when the robot is to be used as an actuator for other purposes, for example, rehabilitation.

C. Comparison with Previous Studies

As we are aware of no previous multivariable ankle impedance study by other research groups, direct comparison is not available. Instead, we compared our results in IE and DP with previous single DOF studies. Our results confirm previous findings that DP impedances at different levels of tonic activity are well approximated by a second-order model consisting of rotational inertia, viscosity, and stiffness [6]. Identified inertia and viscous parameters (Table II) were consistent with previously reported values [10], [32]. Identified stiffness parameters also fell within the range of previous findings, though that range was broad even with comparable muscle activation; for example, estimates based on oscillatory torque perturbations [1] reported stiffness values a few times lower than those using stochastic displacement perturbations [8]. In general, stiffness estimation is sensitive to measurement conditions, including ankle position, input perturbation type, and the amplitude and duration of perturbation [6]. Further investigation of how stochastic torque perturbations and displacement perturbations affect joint impedance is desirable, as emphasized by [26], [41]. We also observed that viscous and stiffness parameters increased with muscle activation, consistent with previous findings [6], [11]. Similarly, IE impedances were also well explained by second-order models, and viscous and stiffness parameters increased with muscle activation. While measurements in our study were made seated, without weight bearing, previous studies were performed either in an upright bipedal weight-bearing stance [14] or standing while bearing different weights [15]. Although no direct comparison at matched muscle activation was possible, our results at

25%–30% MVC agreed with results while standing from [14] and while bearing 30% of body weight [15].

D. Multivariable Dynamic Study Versus Multivariable Static Study

Multivariable dynamic and static studies provide two unique opportunities to investigate ankle impedance beyond single DOF studies. The dynamic studies presented in this paper and our previous study [24] enabled characterization of ankle impedance over a wide range of frequencies, not limited to static conditions. One weakness of this method is that a single estimate of impedance is made at one position at a time, requiring multiple separate measurements to characterize impedance over a wide ROM. The use of LTI system identification is another limitation, but this method can be extended to time-varying system identification [42], [43] or nonlinear system identification while retaining the current experimental setup using a wearable ankle robot actuating multiple DOFs. On the other hand, in the static studies [20], [21], a precise vector field describing a nonlinear torque-angle relationship at the ankle was identified, from which local stiffness can be calculated at any point in the displacement field over a wide ROM. However, that method is confined to the static component. Since each characterization method, dynamic and static, has its advantages and disadvantages, different methods may be appropriate for different applications. The measurement time for each method is short (< 1 minute), and the same experimental setup can be used for both. Thus, rather than relying on either method alone, it is feasible to use both methods to obtain a fuller characterization of ankle impedance.

E. Summary

Summarizing, despite the internal complexities of the ankle, its multivariable mechanical impedance was remarkably simple, at least for our young healthy subjects and in the context of this experiment; the coupling between IE and DP was small so that IE and DP impedances can be treated independently; IE and DP impedances were largely consistent with a second-order model; the characteristic "peanut" shaped anisotropy of ankle impedance was maintained over a wide range of frequencies; and the relationship between muscle activation and ankle stiffness in the 2-D space was highly linear. Considering that multiple ankle muscles acting in both the sagittal and frontal planes affect ankle behavior in both DOFs and intra- and inter-muscular reflex feedback may also contribute to the modulation of ankle impedance [44], it is surprising that multivariable ankle impedance is externally simple even with considerable muscle activation. Interestingly, many of these simple behaviors were also observed in the relaxed study [24], and we venture to speculate that the neuro-muscular system may have evolved towards maintaining a simple ankle impedance, minimally coupling sagittal and frontal plane motions, even when muscles were active.

Although this study only reports inter-subject variability, intra-subject variability analysis will also add value to provide better objective measures of ankle joint properties in multiple DOFs. With a test-retest paradigm as in a previous single DOF study [32], we can quantify intra-subject variability of multivariable ankle impedance, more specifically the variability of ankle parameters in joint coordinates, anisotropy of ankle impedance, and its relationship to muscle activation. That future study may support the use of quantitative measures of multivariable ankle impedance for assessment of pathophysiological ankle behaviors and monitoring of rehabilitation progress.

F. Implications for Clinical Applications

While exploiting these simple characteristics of ankle impedance may be a good strategy for most healthy humans to interact naturally with a dynamically changing physical world, neurologically impaired patients may not enjoy this simplicity due to abnormal muscle tone or reflex feedback arising from lesions of central motor pathways, as well as possible severe alteration of biomechanical properties. Previous studies on patients with several types of neurological disorders demonstrated that pathophysiological ankle impedance substantially deviated from the unimpaired baseline. Static measurements with chronic stroke patients exhibiting spastic hypertonia showed significant alteration of passive ankle stiffness in dorsiflexion and plantarflexion [2], [45]. Another study of stroke survivors with active muscles revealed that although the passive stiffness of the paretic ankle was elevated above the unimpaired baseline, its compliance did not change with muscle activation [5]. Stroke patients also exhibited higher reflex and intrinsic stiffness in the spastic/paretic ankle than on the nonparetic side [46]. Besides stroke patients, patients with spinal cord injury and multiple sclerosis also showed higher reflex stiffness and/or increased nonreflex mediated stiffness (passive plus active stiffness) [3], [47], [48]. More recently, passive ankle stiffness in chronic hemiparetic stroke survivors was measured in both IE and DP directions; however, that study did not assess the coupling between DOFs and was limited to the quantification of static ankle impedance [19].

Although these previous studies have quantified abnormal properties of the impaired ankle, other important pathophysiological features, not available from single DOF or uncoupled multi-DOF studies, may be unveiled by multivariable studies. The multivariable dynamic study we report here and in forthcoming papers based on [49], addressing inter-muscular reflex feedback around the ankle and time-varying ankle impedance in more general motor conditions (for example human walking), promises a more comprehensive characterization of pathophysiological behaviors, and ultimately better tools to quantify impairment and design procedures for the rehabilitation of patients' motor skills.

APPENDIX

Joint stiffness is determined by muscle generated stiffness and kinematic stiffness due to nonlinear musculo-tendon kinematics [37], [38]. For example, in a single DOF, the derivative of muscle length ($l = l(\theta)$) with respect to joint angle (θ) determines the moment arms (r) of the muscle force (f) about the joint ($r(\theta) = \partial l/\partial\theta$), where joint torque $\tau = r(\theta)f$. Hence, the stiffness is defined as$K = \partial\tau/\partial\theta = r(\theta)(\partial f/\partial l)(\partial l/\partial\theta) + (\partial r/\partial\theta)f$. The first term in this expression is the muscle stiffness times the square of the moment arm. The second term is

due to the nonlinear kinematics and is proportional to muscle force. Because of human endo-skeletal anatomy, for modest displacements of the joint from its neutral posture this "kinematic stiffness" is negative. If sufficiently large muscle forces could be exerted without a sufficiently large increase in muscle stiffness, joint stiffness would become negative, i.e., statically unstable. In this study, ankle positions under the given experimental conditions were tightly constrained and the variation of muscle moment arms was expected to be very small, while derivatives of muscle moment arms, which determine the kinematic stiffness, need not be.

ACKNOWLEDGMENT

N. Hogan and H. I. Krebs are co-inventors of the MIT patents for the robotic devices used in this study. They hold equity positions in Interactive Motion Technologies, Inc., the company that manufactures this type of technology under license to MIT.

REFERENCES

[1] G. C. Agarwal and G. L. Gottlieb, "Oscillation of human ankle joint in response to applied sinusoidal torque on foot," *J. Physiol. London*, vol. 268, no. 1, pp. 151–176, 1977.

[2] S. G. Chung, E. van Rey, Z. Q. Bai, E. J. Roth, and L. Q. Zhang, "Biomechanic changes in passive properties of hemiplegic ankles with spastic hypertonia," *Arch. Phys. Med. Rehabil.*, vol. 85, no. 10, pp. 1638–1646, 2004.

[3] J. Lorentzen, M. J. Grey, C. Crone, D. Mazevet, F. Biering-Sorensen, and J. B. Nielsen, "Distinguishing active from passive components of ankle plantar flexor stiffness in stroke, spinal cord injury and multiple sclerosis," *Clin. Neurophysiol.*, vol. 121, no. 11, pp. 1939–1951, 2010.

[4] T. Sinkjaer, E. Toft, S. Andreassen, and B. C. Hornemann, "Muscle-stiffness in human ankle dorsiflexors—Intrinsic and reflex components," *J. Neurophysiol.*, vol. 60, no. 3, pp. 1110–1121, 1988.

[5] S. J. Rydahl and B. J. Brouwer, "Ankle stiffness and tissue compliance in stroke survivors: A validation of myotonometer measurements," *Arch. Phys. Med. Rehabil.*, vol. 85, no. 10, pp. 1631–1637, 2004.

[6] R. E. Kearney and I. W. Hunter, "System-identification of human joint dynamics," *Crit. Rev. Biomed. Eng.*, vol. 18, no. 1, pp. 55–87, 1990.

[7] R. E. Kearney and I. W. Hunter, "Dynamics of human ankle stiffness—Variation with displacement amplitude," *J. Biomechan.*, vol. 15, no. 10, pp. 753–756, 1982.

[8] I. W. Hunter and R. E. Kearney, "Dynamics of human ankle stiffness—Variation with mean ankle torque," *J. Biomechan.*, vol. 15, no. 10, pp. 747–752, 1982.

[9] P. L. Weiss, R. E. Kearney, and I. W. Hunter, "Position dependence of ankle joint dynamics. 1. Passive mechanics," *J. Biomechan.*, vol. 19, no. 9, pp. 727–735, 1986.

[10] P. L. Weiss, R. E. Kearney, and I. W. Hunter, "Position dependence of ankle joint dynamics. 2. Active mechanics," *J. Biomechan.*, vol. 19, no. 9, pp. 737–751, 1986.

[11] P. L. Weiss, I. W. Hunter, and R. E. Kearney, "Human ankle joint stiffness over the full range of muscle activation levels," *J. Biomechan.*, vol. 21, no. 7, pp. 539–544, 1988.

[12] R. E. Kearney, R. B. Stein, and L. Parameswaran, "Identification of intrinsic and reflex contributions to human ankle stiffness dynamics," *IEEE Trans. Biomed. Eng.*, vol. 44, no. 6, pp. 493–504, Jun. 1997.

[13] M. M. Mirbagheri, H. Barbeau, and R. E. Kearney, "Intrinsic and reflex contributions to human ankle stiffness: Variation with activation level and position," *Exp. Brain Res.*, vol. 135, no. 4, pp. 423–436, 2000.

[14] S. M. Zinder, K. P. Granata, D. A. Padua, and B. M. Gansneder, "Validity and reliability of a new in vivo ankle stiffness measurement device," *J. Biomechan.*, vol. 40, no. 2, pp. 463–467, 2007.

[15] A. Saripalli and S. Wilson, "Dynamic ankle stability and ankle orientation," in *Proc. 7th Symp. Footwear Biomechan.*, Cleveland, OH, 2005, pp. 1–2.

[16] J. Mizrahi, Y. Ramot, and Z. Susak, "The dynamics of the subtalar joint in sudden inversion of the foot," *J. Biomech. Eng.*, vol. 112, no. 1, pp. 9–14, 1990.

[17] J. Perry, *Gait Analysis: Normal and Pathologic Functions*. Thorofare, NJ: Slack, 1992.

[18] A. Roy, H. I. Krebs, D. J. Williams, C. T. Bever, L. W. Forrester, R. M. Macko, and N. Hogan, "Robot-aided neurorehabilitation: A novel robot for ankle rehabilitation," *IEEE Trans. Robot.*, vol. 25, no. 3, pp. 569–582, Jun. 2009.

[19] A. Roy, H. I. Krebs, C. T. Bever, L. W. Forrester, R. F. Macko, and N. Hogan, "Measurement of passive ankle stiffness in subjects with chronic hemiparesis using a novel ankle robot," *J. Neurophysiol.*, vol. 105, no. 5, pp. 2132–2149, 2011.

[20] H. Lee, P. Ho, M. A. Rastgaar, H. I. Krebs, and N. Hogan, "Multivariable static ankle mechanical impedance with relaxed muscles," *J. Biomechan.*, vol. 44, no. 10, pp. 1901–1908, 2011.

[21] H. Lee, P. Ho, M. A. Rastgaar, H. I. Krebs, and N. Hogan, "Multivariable static ankle mechanical impedance with active muscles," *IEEE Trans. Neural Syst. Rehabil. Eng.*, vol. 22, no. 1, pp. 44–52, Jan. 2014.

[22] H. Lee, T. Patterson, J. Ahn, D. Klenk, A. Lo, H. I. Krebs, and N. Hogan, "Static ankle impedance in stroke and multiple sclerosis: A feasibility study," in *Proc. Annu. Int. Conf. IEEE EMBC*, 2011, pp. 8523–8526.

[23] H. Lee, H. I. Krebs, and N. Hogan, "A novel characterization method to study multivariable human joint mechanical impedance," in *Proc. 4th Int. IEEE Biomed. Robot. Biomechatron. Conf,*, Rome, Italy, 2012, pp. 1524–1529.

[24] H. Lee, H. I. Krebs, and N. Hogan, "Multivariable dynamic ankle mechanical impedance with relaxed muscles," *IEEE Trans. Neural Syst. Rehabil. Eng.*, 2014, to be published.

[25] M. A. Rastgaar, P. Ho, H. Lee, H. I. Krebs, and N. Hogan, "Stochastic estimation of multi-variable human ankle mechanical impedance," in *Proc. ASME 2009 Dynamic Syst. Control Conf.*, Hollywood, CA, 2009, pp. 957–959.

[26] E. de Vlugt, A. C. Schouten, and F. C. T. van der Helm, "Closed-loop multivariable system identification for the characterization of the dynamic arm compliance using continuous force disturbances: A model study," *J. Neurosci. Methods*, vol. 122, no. 2, pp. 123–140, 2003.

[27] E. A. Clancy and N. Hogan, "Relating agonist-antagonist electromyograms to joint torque during isometric, quasi-isotonic, nonfatiguing contractions," *IEEE Trans. Biomed. Eng.*, vol. 44, no. 10, pp. 1024–1028, Oct. 1997.

[28] J. Montgomery and D. Avers, *Daniels and Worthingham's Muscle Testing: Techniques of Manual Examination*, 8th ed. Philadelphia, PA: Saunders, 2007.

[29] J. Bendat and A. Piersol, *Random Data: Analysis and Measurement Process*, 4th ed. New York: Wiley, 2010.

[30] E. J. Perreault, R. F. Kirsch, and A. M. Acosta, "Multiple-input, multiple-output system identification for characterization of limb stiffness dynamics," *Biol. Cybern.*, vol. 80, no. 5, pp. 327–337, 1999.

[31] A. d'Avella and E. Bizzi, "Shared and specific muscle synergies in natural motor behaviors," *Proc. Nat. Acad. Sci. USA*, vol. 102, no. 8, pp. 3076–3081, 2005.

[32] R. E. Kearney, P. L. Weiss, and R. Morier, "System-identification of human ankle dynamics—Intersubject variability and intrasubject reliability," *Clin. Biomechan.*, vol. 5, no. 4, pp. 205–217, 1990.

[33] E. Kandel, J. Schwartz, and T. Jessell, *Principles of Neural Science*, 5th ed. New York: McGraw-Hill Medical, 2000.

[34] L. Q. Zhang and W. Z. Rymer, "Simultaneous and nonlinear identification of mechanical and reflex properties of human elbow joint muscles," *IEEE Trans. Biomed. Eng.*, vol. 44, no. 12, pp. 1192–1209, Dec. 1997.

[35] R. R. Carter, P. E. Crago, and M. W. Keith, "Stiffness regulation by reflex action in the normal human hand," *J. Neurophysiol.*, vol. 64, no. 1, pp. 105–118, 1990.

[36] N. Mrachacz-Kersting and T. Sinkjaer, "Reflex and non-reflex torque responses to stretch of the human knee extensors," *Exp. Brain Res.*, vol. 151, no. 1, pp. 72–81, 2003.

[37] N. Hogan, , J. Winters and S. Woo, Eds., "Mechanical Impedance of Single- and Multi-Articular System," in *Multiple Muscle Systems: Biomechanics and Movement Organization*. New York: Springer-Verlag, 1990, pp. 149–164.

[38] R. Shadmehr and M. A. Arbib, "A mathematical-analysis of the force-stiffness characteristics of muscles in control of a single joint system," *Biol. Cybern.*, vol. 66, no. 6, pp. 463–477, 1992.

[39] D. H. Odonoghue, Treatment of Injuries to Athlethes Saunders. Philadelphia, PA, 1984.

[40] J. F. Baumhauer, D. M. Alosa, P. A. F. H. Renstrom, S. Trevino, and B. Beynnon, "A prospective-study of ankle injury risk-factors," *Am. J. Sports Med.*, vol. 23, no. 5, pp. 564–570, 1995.

[41] F. C. T. van der Helm, A. C. Schouten, E. de Vlugt, and G. G. Brouwn, "Identification of intrinsic and reflexive components of human arm dynamics during postural control," *J. Neurosci. Methods*, vol. 119, no. 1, pp. 1–14, 2002.
[42] H. Lee and N. Hogan, "Investigation of human ankle mechanical impedance during locomotion using a wearable ankle robot," in *Proc. 2013 IEEE Int. Conf. Robot. Automat.*, Karlsruhe, Germany, 2013, pp. 2636–2641.
[43] H. Lee and N. Hogan, "Human ankle mechanical impedance during locomotion," *IEEE Trans. Neural Syst. Rehabil. Eng.*, to be published.
[44] A. Prochazka, "Proprioceptive Feedback and Movement Regulation," in *Comprehensive Physiology*. New York: Wiley., 1996.
[45] S. G. Chung, E. Van Rey, Z. Q. Bai, W. Z. Rymer, E. J. Roth, and L. Q. Zhang, "Separate quantification of reflex and nonreflex components of spastic hypertonia in chronic hemiparesis," *Arch. Phys. Med. Rehabil.*, vol. 89, no. 4, pp. 700–710, 2008.
[46] M. M. Mirbagheri, L. Alibiglou, M. Thajchayapong, and W. Z. Rymer, "Muscle and reflex changes with varying joint angle in hemiparetic stroke," *J. Neuroeng. Rehabil.*, vol. 5, p. 6, 2008.
[47] M. M. Mirbagheri, H. Barbeau, M. Ladouceur, and R. E. Kearney, "Intrinsic and reflex stiffness in normal and spastic, spinal cord injured subjects," *Exp. Brain Res.*, vol. 141, no. 4, pp. 446–459, 2001.
[48] T. Sinkjaer, E. Toft, K. Larsen, S. Andreassen, and H. J. Hansen, "Non-reflex and reflex mediated ankle joint stiffness in multiple-sclerosis patients with spasticity," *Muscle Nerve*, vol. 16, no. 1, pp. 69–76, 1993.
[49] H. Lee, "Quantitative characterization of multi-variable human ankle mechanical impedance," Ph.D. dissertation, Dept. Mechan. Eng., Massachusetts Inst.Technol, Cambridge, 2013.

Hyunglae Lee (M'14) received the B.S. (*summa cum laude*) and the M.S. degrees in mechanical engineering from Seoul National University, Seoul, South Korea, in 2002 and 2004, respectively, and the Ph.D. degree in mechanical engineering from the Massachusetts Institute of Technology, Cambridge, MA, USA, in 2013. He is currently a postdoctoral fellow at the Sensory Motor Performance Program, Rehabilitation Institute of Chicago, Chicago, IL, USA.

He also worked at Korea Institute of Science and Technology (2006–2008) and LG Electronics (2004–2006) as a researcher in the field of human–computer interaction, human–robot interaction, and mechanical design. His current research interest includes system identification, rehabilitation robotics, biomechanics, and neuromotorcontrol.

Dr. Lee is a recipient of Samsung Scholarship.

Hermano Igo Krebs (F'14) joined the Mechanical Engineering Department, Massachusetts Institute of Technology, Cambridge, MA, USA, in 1997, where he is a Principal Research Scientist—Newman Laboratory for Biomechanics and Human Rehabilitation. He also holds an affiliate position as an Adjunct Professor at University of Maryland School of Medicine, Department of Neurology and the Division of Rehabilitative Medicine. He is one of the founders of Interactive Motion Technologies, a start-up developing robotics for rehabilitation. He is one of the pioneers of rehabilitation robotics and his goal is to revolutionize rehabilitation medicine by applying robotics to assist, enhance, and quantify rehabilitation. His efforts led to the American Heart Association to endorse in its 2010 guidelines for stroke care the use of robots for upper extremity rehabilitation. Similar endorsement was issued by the Veterans Administration later in that same year.

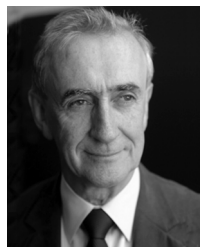

Neville Hogan received the Dip.Eng. (with distinction) from Dublin Institute of Technology, Dublin, Ireland, and the M.S., M.E. and Ph.D. degrees from the Massachusetts Institute of Technology, Cambridge, MA, USA.

He is Sun Jae Professor of Mechanical Engineering and Professor of Brain and Cognitive Sciences at the Massachusetts Institute of Technology (MIT), Cambridge, MA, USA. Following industrial experience in engineering design, he joined MIT's School of Engineering faculty in 1979 and has served as Head and Associate Head of the MIT Mechanical Engineering Department's System Dynamics and Control Division. He is Director of the Newman Laboratory for Biomechanics and Human Rehabilitation and a founder and Director of Interactive Motion Technologies, Inc. His research interests include robotics, motor neuroscience, and rehabilitation engineering, emphasizing the control of physical contact and dynamic interaction.

Prof. Hogan has been awarded Honorary Doctorates from Delft University of Technology and Dublin Institute of Technology; the Silver Medal of the Royal Academy of Medicine in Ireland; the Henry M. Paynter Outstanding Investigator Award, and the Rufus T. Oldenburger Medal from the Dynamic Systems and Control Division of the American Society of Mechanical Engineers.